Article

Damage Characteristics and Energy Evolution of Bituminous Sandstones under Different Cyclic Amplitudes

Xiaoyu Lu [1,2,3], Ruipeng Qin [1,2,*], Chunliang Dong [1,2,3] and Chaotao Fan [1,2]

1 State Key Laboratory of Mining Response and Disaster Prevention and Control in Deep Coal Mines, Anhui University of Science and Technology, Huainan 232001, China; luxy@aust.edu.cn (X.L.); dongchunliang@163.com (C.D.); fanchaotaogq@163.com (C.F.)
2 School of Civil Engineering and Architecture, Anhui University of Science and Technology, Huainan 232001, China
3 School of Mechanics and Optoelectronic Physics, Anhui University of Science and Technology, Huainan 232001, China
* Correspondence: austqin@163.com

Abstract: In many underground engineering projects, rocks are often subjected to cyclic loading and unloading, such as repeated excavation of roadway surrounding rock, which will lead to damage to underground rocks, and the energy of rocks also changes. Therefore, to study the energy evolution and damage characteristics of rocks under cyclic loading and unloading, different cyclic loading and unloading tests of bituminous sandstones under constant amplitude were conducted. Under cyclic loading and unloading, the lower limit stress was 40% of the rock peak intensity, the cyclic amplitude was 20–40% of the peak intensity, and the number of loading–unloading cycles was 10–30. The quantitative characterization of the damage degrees of bituminous sandstone was realized by the ultrasonic wave velocity and elasticity modulus methods. The energy evolution and damage characteristics of bituminous sandstone under different amplitudes and number of loading–unloading cycles were investigated through the energy dissipation method. Results showed that under cyclic loading and unloading, the ultrasonic wave velocity and elasticity modulus of bituminous sandstone decreased gradually; The damage variable shows a trend of rapid and then stable growth and has a power function relationship with the number of cycles; The input energy density and dissipation energy density curves were in L-shaped distribution, whereas the elastic energy density remained stable. The results of this study can provide some theoretical references to underground engineering construction.

Keywords: cyclic loading and unloading; rock damage; energy evolution; damage characteristics

1. Introduction

With the rapid national economic development and increasing infrastructure inputs, many large engineering projects have been launched. These projects are often influenced by cyclic loading and unloading. For example, the repeated excavation of surrounding rocks [1,2] in a roadway and continuous construction and geological conformation movement in underground projects may bring a series of hidden hazards that may influence the safety and stability of projects and may even cause construction disasters. Therefore, the damage characteristics and energy evolution of rocks under cyclic loading and unloading must be studied in the field of rock engineering.

Recently, scholars in the field of rock mechanics have conducted numerous studies on the damage characteristics and energy evolution of rocks under cyclic loading and unloading and achieved substantial results. Peng et al. [3] studied the energy evolution mechanism of coal rocks under different loading and unloading modes and revealed the cyclic hysteresis phenomena and the relationship between the stress and damage dissipation of coal rocks under cyclic loading and unloading. Pei et al. [4] studied the energy evolution law of

granite during the entire process under cyclic loading and unloading and analyzed the energy and mechanical properties of granite under different confining pressures. Liu et al. [5] studied the mechanical properties and energy evolution laws of hard rocks under different confining pressure during the damage process and disclosed the relationship between the energy density of rocks and confining pressure. Li et al. [6] conducted a uniaxial cyclic loading test of sandstones and summarized the variation laws of deformation, the deformation modulus and lateral expansion coefficient of sandstones, and the failure modes of rocks under cyclic loading and unloading. Jiang et al. [7] conducted a triaxial cyclic loading and unloading test of natural shale and analyzed the deformation characteristics, energy evolution, and damping characteristics of natural shale under different confining pressures. Deng et al. [8] studied the energy evolution of sandstones during uniaxial cyclic loading and unloading and discussed the variation laws of energy and parameters during loading and unloading. Miao et al. [9] analyzed the evolutionary laws of dissipated energy, friction energy dissipation, and breakage energy of granite under cyclic loads. Zhang et al. [10] conducted a triaxial cyclic loading and unloading test of coal rocks under the collaborative action of confining pressure and gas pressure and constructed a damage constitutive model based on energy dissipation. They found variation laws of energy evolution and damages of coal rocks under different confining and gas pressures. Zhao et al. [11] studied the damage deformation and energy characteristics of rocks through triaxial cyclic loading and unloading and revealed the relationship between damages and residual deformation. Xu et al. [12] conducted a cyclic loading and unloading test and constant-load fatigue test and analyzed the variation laws of the energy dissipation of mudstones and their damage characteristics by studying the energy evolution and damage characteristics of saturated rocks under cyclic loads. Jing et al. [13] compared the energy variation laws of saturated rock materials under different cyclic loading and unloading modes. Moon et al. [14] carried out a series of bedrock depth detection in order to detect earthquake disasters and develop underground. Based on surface wave technology, microtremor array measurement, and microtremor measurement, four measurement methods of bedrock depth in Singapore Bukit Timah granite were found, and it was proved that a non-invasive surface wave detection method could be used for bedrock detection. Oteuil et al. [15] conducted a series of laboratory tests to make deep foundation piles safer. Through numerical calculation, it is found that as long as the numerical results are correct, the safety design can be realized with several soil parameters.

Although the above research has achieved rich research results, it mainly focuses on the cyclic loading and unloading test under a single amplitude, and there are few studies on the damage characteristics and energy evolution under different amplitude cyclic loading and unloading, especially the rock of bituminous sandstones. Therefore, this paper takes bituminous sandstones as the research object, studies the energy evolution law of bituminous sandstones under different cyclic amplitude loading and unloading, and uses three methods to characterize the damage degree of bituminous sandstones after damage, that is, ultrasonic wave velocity method, elasticity modulus method, and energy dissipation method. The damage characteristics of bituminous sandstones under different cyclic loading and unloading amplitudes and cycles are analyzed. It provides a certain reference for the safe construction of underground bituminous sandstone rock mass engineering.

2. Sample Preparation and Experimental Methods

2.1. Sample Preparation

In this experiment, bituminous sandstones of the same rock stratum, which have similar internal structures and no evident deflects and surface fractures, were used as samples. According to the method suggested by the International Rock Mechanics Experiment [16], the cores of bituminous sandstones were collected, cut, and ground into cylinder-standard samples with a diameter of 50 mm and a height of 100 mm. The degree of parallelism of the upper and lower end surfaces were controlled within ±0.02 mm (Figure 1). The

average comprehensive strength of samples was 54 MPa. The longitudinal wave velocity of bituminous sandstones was tested using an MC-6310 nonmetal ultrasonic detector to eliminate samples with great discreteness.

Figure 1. Bituminous sandstone specimens.

2.2. Experimental Apparatus and Experimental Scheme

The experimental apparatus used in this study was an RMT rock mechanical tester produced by Changchun Zhaoyang Instrument Co., Ltd. (Changchun, China). Uniaxial cyclic loading and unloading were applied. According to the literature research [17], it is found that the rock reaches 40% σ_c, which may be affected by different damage variables. Due to the high unloading point, there may be sudden rock failure, So choose 60% σ_c to 80% σ_c serves as the unloading point. The lower limit stress was 40% of the peak intensity, and the loading and unloading rates were 500 N/s. The constant amplitudes of cyclic loading and unloading involved three types:

(1) The amplitude was 20%, and the number of loading–unloading cycles was 10, 20, and 30, respectively.
(2) The amplitude was 30%, and the number of loading–unloading cycles was 10, 20, and 30, respectively.
(3) The amplitude was 40%, and the number of loading–unloading cycles was 10, 20, and 30, respectively.

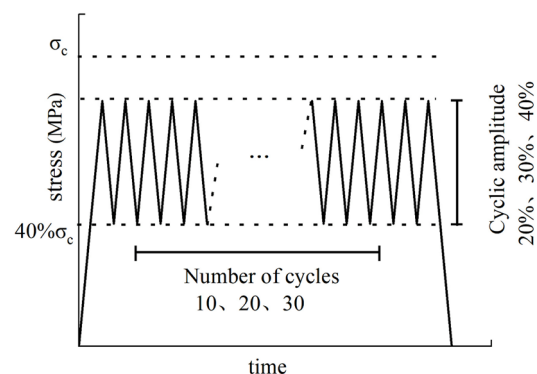The loading and unloading routes of the bituminous sandstones are shown in Figure 2.

Figure 2. Equal-width loading and unloading paths.

3. Quantitative Characterization of Bituminous Sandstone Damages under Cyclic Loading and Unloading

3.1. Ultrasonic Wave Velocity Method

After the cyclic loading and unloading effect of the rock samples, the expansion and extension of microcracks inside must occur to influence the propagation speed of elastic waves inside rocks. Hence, the changes in ultrasonic velocity can reflect the damage

conditions of rocks. In this study, longitudinal wave velocity was used to define the damage variable of bituminous sandstones [18–20]. In order to provide readers with a better understanding of the specific details of using the acoustic velocity method to calculate damage variables, the calculation formula is now listed as follows:

$$D_V = 1 - \frac{V^2}{V_0^2},$$ (1)

where V_0 is the longitudinal wave velocity before the loading–unloading induced damages of rocks, and V is the longitudinal wave velocity after damages.

In accordance with the wave velocity of test samples, the damage variable (D_V) defined by the longitudinal wave velocity was calculated using Equation (1). Results are shown in Table 1.

Table 1. The longitudinal wave velocity and damage of samples (↓: lower).

Sample Number	Lower Limit of Cycle	Cyclic Amplitude (f)	Number of Cycles	V_0 (m/s)	V (m/s)	Wave Speed Reduction ↓	D_V
①			10		2210	7.1%	0.138
②		20% σ_c	20		2195	7.8%	0.149
③			30		2187	8.1%	0.156
④			10		2135	10.3%	0.195
⑤	40% σ_c	30% σ_c	20	2380	2127	10.6%	0.201
⑥			30		2122	10.8%	0.205
⑦			10		2045	14.1%	0.262
⑧		40% σ_c	20		2034	14.5%	0.269
⑨			30		2030	14.7%	0.273

Table 1 shows that given the same number of loading–unloading cycles, the damage of samples increased with the increase in loading and unloading amplitude from 0.138 to 0.262, from 0.149 to 0.269, and from 0.156 to 0.273. However, the trend of damage increase decreased gradually. The damage variable of Sample ① increased by 41% compared with that of Sample ④. The damage variable of Sample ④ increased only by 34% compared with those of Sample ⑦. Similarly, samples ②, ⑤ and ⑧ increased by 35% and 34%, respectively; samples ③, ⑥ and ⑨ also have similar rules.

Given the same loading and unloading amplitude, the damage variable increased with the increase in the number of loading–unloading cycles. However, the influence of the number of loading–unloading cycles was considerably weaker than those of the loading and unloading amplitude. The damage variable increased only by 8% and 4.7% for Samples ①–③, 3.1% and 2% for Samples ④–⑥, and 2.7% and 1.5% for Samples ⑦–⑨, which had the lowest growth rate.

Overall, the effects of loading and unloading amplitudes on sample damages were stronger than those of the number of loading–unloading cycles. In particular, the growth rate of damages was considerably under a small amplitude and a low number of cycles, which were attributed to the continuous connection and extension of cracks in rocks. However, with the increase in the number of loading–unloading cycles, the expandable microcracks decreased sharply due to limitation by the constant loading and unloading amplitudes, thus slowing down the growth of damages.

3.2. Elasticity Modulus Method

Based on continuum theory, studying rock damage from the macroscopic perspective is the initial idea to study damage mechanics. Specifically, the elasticity modulus method is relatively universal. The calculation formula is [21]:

$$D_E = 1 - \frac{E}{E_0},\qquad(2)$$

where E is the elasticity modulus after sample damages, determined by the value corresponding to the last unloading curve under cyclic loading and unloading; E_0 is the elasticity modulus before damages, which is determined by the value corresponding to the first loading curve under cyclic loading and unloading.

The damage variable (D_E) of the rock samples under cyclic loading and unloading was calculated using Equation (2). Results are shown in Table 2.

Table 2. The elastic modulus and damage of samples.

Sample Number	E_0 (GPa)	E (GPa)	Reduction in Elastic Modulus	D_E
①		7.81	15.2%	0.133
②		7.62	18.1%	0.153
③		7.51	19.8%	0.166
④		7.31	23.1%	0.189
⑤	9	7.15	25.9%	0.206
⑥		7.05	27.7%	0.217
⑦		6.51	38.2%	0.277
⑧		6.32	42.4%	0.298
⑨		6.22	43.9%	0.309

Table 2 shows that after cyclic loading and unloading, the elasticity modulus of rock samples decreased. In particular, the elasticity modulus was decreased to the maximum extent by 43.9% when the amplitude reached 40% σ_c.

Given the sample loading and unloading amplitudes, the damage variable of rock samples increased from 0.133 to 0.166 with the increase in the number of loading–unloading cycles (f = 20% σ_c), from 0.189 to 0.217 (f = 30% σ_c), and from 0.277 to 0.309 (f = 40% σ_c). Except for sample ①, damages of other rock samples defined by the elasticity modulus method were slightly higher than those determined by the longitudinal wave velocity method. Given the same number of loading–unloading cycles, the growth rate of rock damages increased with the increase in loading and loading amplitudes, reaching 42% and 46% (n = 10), 35% and 45% (n = 20), and 31% and 42% (n = 30). The damage growth rate in the elasticity modulus method showed better laws than that in the longitudinal wave velocity method. However, the analysis results were generally similar. The increase in amplitudes and the number of cycles facilitate the damage development of rock samples. However, the growth rate of damages increased first and then decreased and finally became stable.

4. Energy Evolution of Bituminous Sandstone under Cyclic Loading and Unloading

Under cyclic loading and unloading, internal cracks started and then connected in rocks, accompanied by energy transformation. According to the first law of thermodynamics [22,23], the power made by the tester to rocks was transformed completely into elastic energy and dissipated energy before thermal energy exchange with the external environment. Elastic energy is the energy absorbed by rocks to recover from deformation during loading, whereas dissipated energy is the energy consumed by rocks to generate damage and plastic strains under cyclic loads.

Hence, the area enclosed by the loading curve and strain (ε) in the cyclic loading and unloading test is the total power made by the tester to test samples; this power

refers to the input energy density (U) of bituminous sandstone. The area enclosed by the unloading curve and strain (ε) is the recoverable elastic energy density (U_e), which is kept in bituminous sandstone. The area between the loading curve and unloading curve, known as the area enclosed by AOBA, is the unrecoverable dissipation energy density (U_d), as shown in Figure 3.
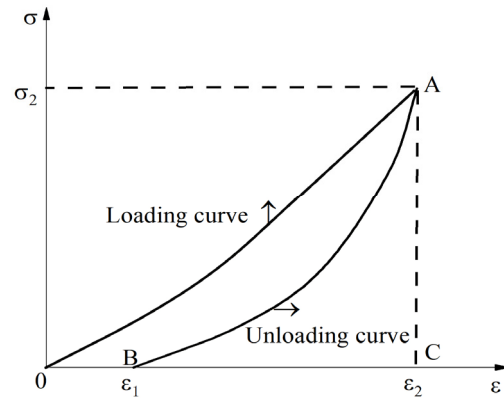

Figure 3. Schematic diagram of loading and unloading energy density calculation.

The expressions of input energy, dissipated energy, and elastic energy are [23–28]

$$U = U_e + U_d, \tag{3}$$

$$U = \int_0^{\varepsilon_2} \sigma_i d\varepsilon_i, \tag{4}$$

$$U_e = \int_{\varepsilon_1}^{\varepsilon_2} \sigma_i d\varepsilon_i, \tag{5}$$

$$U_d = \int_0^{\varepsilon_2} \sigma_i d\varepsilon_i - \int_{\varepsilon_1}^{\varepsilon_2} \sigma_i d\varepsilon_i, \tag{6}$$

where ε_1 is the strain value at the loading stage σ_1, ε_2 is the strain value at the loading stage σ_2, σ_i and ε_i are stress and strains in the ith cyclic loading and unloading, respectively.

According to Equations (3)–(6), the relationship of input energy density, elastic energy density, and dissipation energy density of bituminous sandstones with the number of loading–unloading cycles could be calculated, as shown in Figure 4.

As shown in Figure 4a, when the amplitude of cyclic loading and unloading was 20% σ_c, the initial input energy density was 3.63×10^{-2} MJ/m^{-3}, and it stabilized at 2×10^{-2} MJ/m^{-3} with the increase in the number of cycles, which was decreased by nearly 45% compared with the initial value. When the amplitude of cyclic loading and unloading was 30% σ_c, the initial input energy density was 5.22×10^{-2} MJ/m^{-3}, and it stabilized at 3.1×10^{-2} MJ/m^{-3} with the increase in the number of cycles, which was decreased by nearly 41% compared with the initial value. When the amplitude of cyclic loading and unloading was 40% σ_c, the initial input energy density was 6.93×10^{-2} MJ/m^{-3}, and it stabilized at 4.4×10^{-2} MJ/m^{-3} with the increase in the number of cycles, which was decreased by nearly 37% compared with the initial value. This result indicates that the input energy density increases with the increase in the amplitude of cyclic loading and unloading. When the number of loading–unloading cycles increased, the input energy density was kept stable, except for the first cycle, and its attenuation degree increased continuously in comparison with the previous cycle. Internal cracks must absorb abundant energy for initial connection during the cyclic loading and unloading test under different amplitudes. Hence, the input energy density during the first loading was the highest. Subsequently, some compacted cracks expanded again. During the next loading and unloading cycle, cracks continued to be compacted and expanded. However, the subsequent cyclic loading

and unloading could not initiate new cracks due to the constant amplitude. The original cracks were compacted and closed gradually. As a result, the input energy during loading tended to be stable, and it was kept inside the samples in the form of elastic energy. Input energy density presented an L-shaped distribution with the increase in the number of loading–unloading cycles. Given the cyclic loading and unloading with constant amplitude, increasing the input energy level by increasing the number of loading and unloading cycles is difficult. The elastic energy density was kept stable with the increase in the number of loading–unloading cycles Figure 4b.
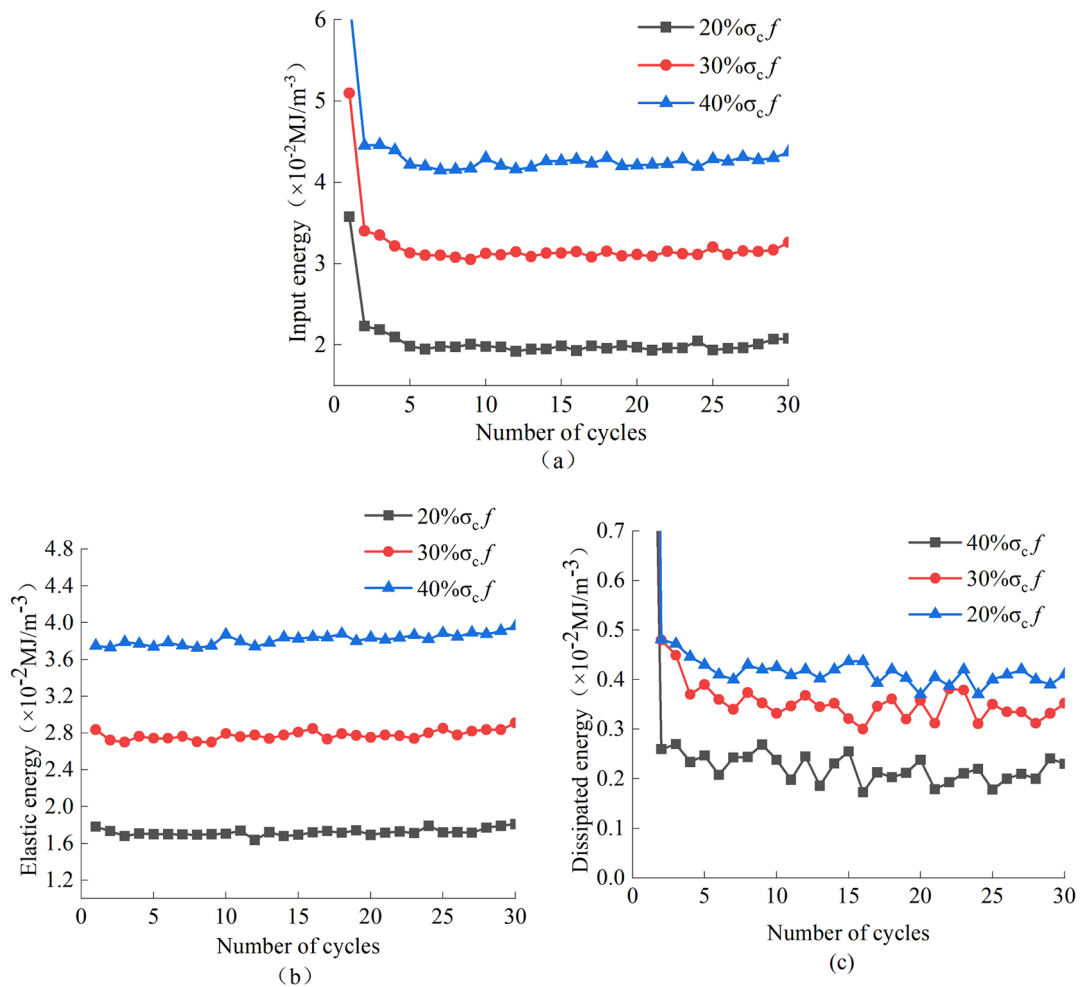

Figure 4. Energy density in relation to the number of cycles. (**a**) Input energy, (**b**) Elastic energy, (**c**) Dissipated energy.

In Figure 4c, the evolutionary laws of dissipation energy density were similar to those of input energy. The dissipation energy density of samples at the first unloading was the highest. Given different cyclic amplitudes, the dissipation energy density values of the first cyclic loading and unloading were 1.93×10^{-2}, 2.45×10^{-2}, and 3.31×10^{-2} MJ/m^{-3}, respectively. As the number of loading–unloading cycles increased, the dissipation energy density stabilized at 0.25×10^{-2}, 0.33×10^{-2}, and 0.42×10^{-2} MJ/m^{-3}, which were all attenuated by approximately 87% in comparison with that during the first cycle. The dissipation energy density exhibited an L-shaped distribution. In summary, the damage to rocks increased the most during the first cycle, and increasing the cyclic amplitude can facilitate the initiation and expansion of cracks in rocks. However, the influence of the number of loading–unloading cycles on the internal damages of rock samples was kept in balance under cyclic loading and unloading with constant amplitudes.

5. Damage Characteristics of Rock Samples Based on Energy Dissipation

In the above text, the energy evolutionary laws of bituminous sandstones under cyclic loading and unloading with constant amplitude were analyzed. Results showed that the energy dissipation of rock samples was a process of internal damage accumulation. Hence, on the basis of rock damage analysis via the longitudinal wave velocity and elasticity modulus methods, cumulative dissipated energy was further applied to study the damage characteristics of bituminous sandstones under different cyclic loading and unloading. The calculation formula is [27]:

$$D_U^i = \frac{U_d^i}{U^i}, \tag{7}$$

$$U_d^i = \sum_{k=1}^{i} U_d^k, \tag{8}$$

$$U_e^i = \sum_{k=1}^{i} U_e^k, \tag{9}$$

$$U^i = U_e^i + U_d^i, \tag{10}$$

where D_U^i is the damage of samples at the ith cyclic loading and unloading; U_d^i, U_e^i, and U^i are cumulative dissipation energy density, cumulative elastic energy density, and cumulative input energy density at the ith cyclic loading and unloading, respectively; U_d^k denotes the kth dissipation energy density; U_e^k refers to the kth elastic energy density.

The variation laws of D_U with the number of loading–unloading cycles under different amplitudes were calculated using Equations (7)–(10), as shown in Figure 5.
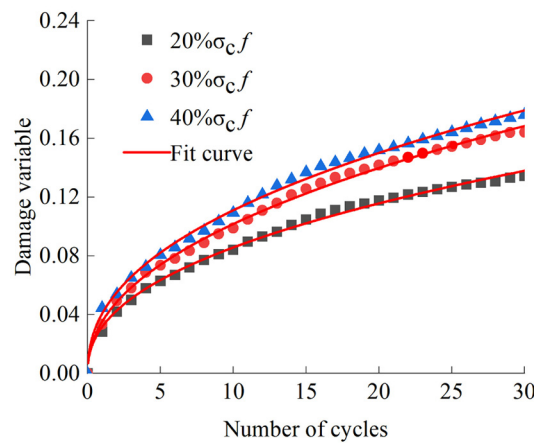

Figure 5. Law of damage evolution.

As shown in Figure 5, the growth rate of damages reached a peak in the first cycle. With the increase in the number of loading–unloading cycles, D_U continued to increase, and the growth rate tended to be stable. In the first several loading–unloading cycles, the internal cracks of bituminous sandstone were connected, and D_U fluctuated considerably. This stage is the fast damage stage. Subsequently, the connection depth of cracks increased to a limited extent due to the influences of cyclic amplitude, and D_U tended to be stable. This stage is the stable damage stage. Moreover, the damage characteristics of bituminous sandstones under different cyclic amplitudes reflected by cumulative dissipated energy were consistent with the results of the ultrasonic wave velocity and elasticity modulus methods. However, the damage degree reflected by cumulative dissipated energy was smaller than those in the ultrasonic wave velocity and elasticity modulus methods.

By fitting the D_U data of samples, the power functional relationship between the damages and the number of loading–unloading cycles was obtained as follows:

$$D_U = ax^b, \tag{11}$$

where D_U is the damage variable; x is the number of loading–unloading cycles; a and b are fitting parameters. Fitting parameters under different cyclic amplitudes are shown in Table 3. Fitting curves are presented in Figure 5. R^2 was higher than 0.99, indicating that the above Equation could reflect damaged evolutionary laws of bituminous sandstones under cyclic loading and unloading with constant amplitude.

Table 3. Specimen damage fitting parameters.

Cyclic Amplitude (*f*)	*a*	*b*	R^2
20% σ_c	0.03168	0.43251	0.99559
30% σ_c	0.03533	0.45916	0.99652
40% σ_c	0.0408	0.43489	0.99541

Based on the above variation laws of sample damages with the number of loading–unloading cycles under different cyclic amplitudes, the damage value of samples could reach 1, and the samples failed in a fatigue test under some cyclic amplitude (loading mode and rate were constant) as long as the loading–unloading cycles were enough. Hence, it can determine the theoretical number of cycles for the fatigue failure of rocks under different cyclic amplitudes by substituting Equation (11) into fitting parameters of samples and $D_U = 1$. This theoretical number of cycles represented the fatigue life (N). According to the calculation, N = 2926.245 when the cyclic amplitude was 20% σ_c. In other words, the bituminous sandstone samples failed at the 2927th loading–unloading cycle when the lower limit of the cyclic amplitudes was 40%, and the cyclic amplitude was 20% σ_c. When the cyclic amplitude was 30% σ_c, N = 1441.74, suggesting that the bituminous sandstone samples failed at the 1442nd loading–unloading cycle when the lower limit of cyclic amplitudes was 40%, and the cyclic amplitude was 30% σ_c. When the cyclic amplitude was 40% σ_c, N = 1077.447, indicating that the bituminous sandstone samples failed at the 1078th loading–unloading cycle when the lower limit of cyclic amplitudes was 40%, and the cyclic amplitude was 40% σ_c.

6. Conclusions

The conclusions can be started as a reference for underground engineering projects.

This paper focuses on the energy evolution and damage characteristics of bituminous sandstones under uniaxial cyclic loading and unloading. The conclusion may not be applicable to other types of rocks. Through the three test methods of damage characteristics and the energy evolution of Bituminous Sandstones under cyclic loading and unloading, the study presents the following conclusions.

1. The ultrasonic wave velocity and elasticity modulus methods show that with the increase in amplitude and the number of loading–unloading cycles, the damage variable of bituminous sandstones increases gradually. The Influences of cyclic amplitude on the damage of bituminous sandstones are stronger than those of the number of loading–unloading cycles. The growth rate of the damage variable increases first, then decreases and finally becomes stable.

2. Under cyclic loading and unloading with constant amplitude, the input energy density of bituminous sandstones increases with the increase in cyclic amplitude. The input energy density and dissipation energy density during the first cycle reach the maximum. With the increase in the number of loading–unloading cycles, the input energy density and dissipation energy density exhibit an L-shaped distribution, whereas the elastic energy density is kept stable.

3. The damage degree of bituminous sandstones increases the most during the first loading–unloading cycle. With the increase in the number of cycles, the damage degree increases, and the growth rate of damages tends to be stable. The damage variable experiences fast damage and stable damage stages.

4. Data fitting of the damage variable of bituminous sandstone samples reveal that the damage variable has a power functional relationship with the number of loading–unloading cycles.

Underground rock engineering will be affected by many factors, seriously endangering people's safety and production, which is of great significance for the study of underground rock problems. Then, the experiment is completed in the laboratory; some conditions are fixed and may have some deviation from the actual underground engineering project. Secondly, this study did not study the damage change and energy evolution of asphalt sandstone under triaxial cyclic loading and unloading. Therefore, it is hoped that more experts and scholars can enrich this research in the future.

Author Contributions: R.Q.: Writing—original draft, methodology; X.L.: methodology, conceptualization; C.D.: revised manuscript, formal analysis; C.F.: formal analysis, resources. All authors have read and agreed to the published version of the manuscript.

Institutional Review Board Statement: Not applicable.

Informed Consent Statement: Not applicable.

Data Availability Statement: The data used to support the findings of this study are included within the article.

Conflicts of Interest: The authors declare no conflict of interest.

References

1. Yang, C.H.; Ma, H.L.; Liu, J.F. Experimental study on deformation characteristics of salt rock under cyclic loading and unloading. *Rock Soil Mech.* **2009**, *30*, 3562–3568. [CrossRef]
2. Zhang, Y.; Miao, S.J.; Guo, Q.F.; Wang, P.T. Microscopic energy evolution and rock burst tendency of granite stress threshold under cyclic loading. *J. Eng. Sci.* **2019**, *41*, 864–873. [CrossRef]
3. Peng, R.D.; Ju, Y.; Gao, F. Energy mechanism analysis of coal rock damage under triaxial cyclic loading and unloading. *J. Chin. Coal Sci.* **2014**, *39*, 245–252. [CrossRef]
4. Pei, F.; Ji, H.G.; Zhang, T.Z. Energy Evolution and Mechanical Features of Granite Subjected to Triaxial Loading-Unloading Cycles. *Adv. Civ. Eng.* **2019**, *2019*, 9871424. [CrossRef]
5. Liu, P.F.; Fan, J.Q.; Guo, J.Q.; Zhu, B.Z. Energy evolution and damage characteristics of granite under triaxial stress loading failure. *Chin. J. High Press. Phys.* **2021**, *35*, 44–53. [CrossRef]
6. Li, X.W.; Yao, Z.S.; Huang, X.Z.; Liu, Z.X.; Zhao, X.; Mu, K.H. Research on deformation and failure characteristics and energy evolution of sandstone under cyclic loading and unloading. *Rock Soil Mech.* **2021**, *42*, 1693–1704. [CrossRef]
7. Jiang, C.B.; Wei, C.; Zhuang, W.J.; Duan, M.K.; Chen, Y.F.; Yu, T. Research on deformation characteristics and energy evolution mechanism of shale under constant amplitude cyclic loading. *J. Rock Mech. Eng.* **2020**, *39*, 2416–2428. [CrossRef]
8. Deng, H.F.; Hu, Y.; Li, J.L.; Wang, Z.; Zhang, X.J.; Hu, A.L. Evolution law of sandstone energy dissipation during cyclic loading and unloading. *J. Rock Mech. Eng.* **2016**, *35* (Suppl. S1), 2869–2875. [CrossRef]
9. Miao, S.J.; Liu, Z.J.; Zhao, X.G.; Huang, Z.J. Energy dissipation and damage characteristics of Beishan granite under cyclic loading. *J. Rock Mech. Eng.* **2021**, *40*, 928–938. [CrossRef]
10. Zhang, Y.; Li, B.B.; Xu, J.; Gao, Z.; Chen, S.; Wang, B. Research on damage evolution characteristics of coal and rock under triaxial compression based on energy dissipation. *J. Rock Mech. Eng.* **2021**, *40*, 1614–1627. [CrossRef]
11. Zhao, C.; Wu, K.; Li, S.; Zhao, J.G. Analysis of rock damage deformation and energy characteristics under cyclic loading. *J. Geotech. Eng.* **2013**, *35*, 90–896.
12. Xu, Y.; Li, C.J.; Zheng, Q.Q.; Ni, X.; Wang, Q.Q. Analysis of energy evolution and damage characteristics of mudstone under cyclic loading and unloading. *J. Rock Mech. Eng.* **2019**, *38*, 2084–2091. [CrossRef]
13. Jing, L.W.; Li, X.S.; Yan, Y.; Peng, S.C.; Li, S.W.; Jing, W. Energy evolution and damage characteristics analysis of saturated rock materials under cyclic loading and unloading. *Min. Res. Dev.* **2022**, *42*, 7. [CrossRef]
14. Moon, S.W.; Subramaniam, P.; Zhang, Y.H.; Vinoth, G.; Taeseo, K. Bedrock depth evaluation using microtremor measurement: Empirical guidelines at weathered granite formation in Singapore. *J. Appl. Geophys.* **2019**, *171*, 103866. [CrossRef]
15. Oteuil1, A.; Oralbek, A.; Mukhamet, T.; Moon, S.W.; Kim, J.; Tokbolat, S.; Satyanaga, A. Robust Analysis and Design of Bored Pile Considering Uncertain Parameters. *Indian Geotech. J.* **2022**, *52*, 720–734. [CrossRef]

16. Zheng, Y.T.; Fu, B.J. *Recommended Method for Rock Mechanics Test by the Laboratory and Fielpndardization Committee of the International Rock Mechanics Society*; Coal Industry Press: Beijing, China, 1982; Volume 12, pp. 32–35.

17. Derek, M.C.; Rolf, C.; Joergen, S. Rock stability considerations for siting and constructing a KBS-2 repository—Based on experiences from Aspo HRL, AECL;s URL, tunneling and mining. *SKB Tech. Rep.* **2001**, *1*, 1–94.

18. Zhao, K.; Jin, J.F.; Wang, X.J.; Zhao, K. Research on the relationship between rock sound velocity, damage, and acoustic emission. *Rock Soil Mech.* **2007**, *2007*, 2105–2109+2114. [CrossRef]

19. Concu, G.; Nicolo, B.D.; Valdes, M. Prediction of Building Limestone Physical and Mechanical Properties by Means of Ultrasonic P-Wave Velocity. *Sci. World J.* **2014**, *2014*, 508073. [CrossRef]

20. Zhang, L.; Zhang, Z.T.; Zhang, R.; Gao, M.Z.; Xie, J. The Ultrasonic P-Wave Velocity-Stress Relationship and Energy Evolution of Sandstone under Uniaxial Loading-Unloading Conditions. *Adv. Mater. Sci. Eng.* **2021**, *2021*, 9921716. [CrossRef]

21. Bo, P. Research on Cumulative Damage of Rocks under Cyclic Dynamic Loads. Master's Thesis, Liaoning University of Science and Technology, Shenyang, China, 2018.

22. Yang, S.; Zhang, N.; Feng, X.W.; Kan, J.G.; Qian, D.Y. Experimental Investigation of Sandstone under Cyclic Loading: Damage Assessment Using Ultrasonic Wave Velocities and Changes in Elastic Modulus. *Shock Vib.* **2018**, *2018*, 7845143. [CrossRef]

23. Xie, H.P.; Ju, Y.; Li, L.Y.; Peng, R.D. Energy mechanism of rock mass deformation and failure process. *J. Rock Mech. Eng.* **2008**, *2008*, 1729–1740. [CrossRef]

24. Xie, H.P.; Peng, R.D.; Ju, Y.; Zhou, H.W. Reliminary study on energy analysis of rock failure. *J. Rock Mech. Eng.* **2005**, *2005*, 2603–2608. [CrossRef]

25. Zhu, A.Q.; Liu, J.F.; Wu, Z.D.; Wang, L.; Xiao, F.K.; Deng, C.F. Energy Dissipation and Damage Evolution Characteristics of Salt Rock under Uniaxial Cyclic Loading and Unloading Tension. *Adv. Civ. Eng.* **2021**, *2021*, 23–28. [CrossRef]

26. Li, X.; Wang, Y.; Xu, S.; Yang, H.; Li, B. Research on Fracture and Energy Evolution of Rock Containing Natural Fractures under Cyclic Loading Condition. *Geofluids* **2021**, *2021*, 9980378. [CrossRef]

27. Chen, X.; Lin, J.; Cao, G.Y.; Yang, Y. Energy evolution characteristics and damage characterization of sandstone under cyclic loading and unloading. *Sci. Tech. Eng.* **2022**, *2022*, 5792–5799.

28. Wen, T.; Tang, H.; Ma, J.; Liu, Y. Energy Analysis of the Deformation and Failure Process of Sandstone and Damage Constitutive Model. *KSCE J. Civ. Eng.* **2019**, *23*, 513–524. [CrossRef]